14th Australasian Fluid Mechanics Conference
Adelaide University, Adelaide, Australia
10-14 December 2001

3D Propagation of CHF/Rewet Front within Rod Bundle in Turbine-Trip-w/o-Bypass Simulation: Experimental and Numerical Investigation based on Porous Media

Zoran V. Stosic[1□], Vladimir D. Stevanovic[✧1□] and Tadashi Iguchi[2]

[1]Framatome ANP GmbH, Bunsenstr. 43, D-91058 Erlangen, Germany
[2]JAERI - Japan Atomic Energy Research Institute, P. O. Box 319-1195, Tokai, Ibaraki, Japan

Abstract

Investigation based on experimental and numerical simulation of three-dimensional transient propagation of a dry-out front within a nuclear fuel rod bundle is performed. It is observed that CHF and rewetting took place at several elevations where the spacers are located. Spreading of CHF across a bundle caused by power increase is quantified and the locus of the dry patches is shown. Due to possible building of vapour zone the CHF spatial propagation has to be carefully analysed in transients.

Introduction

Experimental and numerical investigation of the two-phase flow within nuclear fuel rod bundle under critical power is a difficult task because of the inherent complexity of the two-phase flow, uncertainty of the local conditions that lead to the Critical Heat Flux (CHF) and complex geometry of bundles. The modern fuel rod bundles for Boiling Water Reactors (BWRs) causes significant spatial differences of volumetric heat flux, steam void fraction distribution, mass flux rate and other thermal-hydraulic parameters which are important for the efficient cooling of nuclear fuel rods during normal steady state and transient conditions. This causes the three-dimensional nature of CHF and its spatial complex propagation.

Purpose of this Study

Occurrence of the CHF conditions within the rod bundle is caused by the local partial or complete dry-out of the rod(s). In transient conditions the dry-out front, as the boundary between two-phase mixture and the high quality vapour zone, can propagate both axially and laterally in three-dimensional rod bundle space. The locus of the dry patches in transient conditions can be quite differently positioned than in steady states. Also, the bundle local volumes that undergo into dry-out vary, depending on the nature of the transient, violating in more or less extent the surface of heated rod(s). Furthermore, the CHF does not occur simultaneously across a bundle. It requires typically an increase of about 50% above the critical power (for the same local conditions of pressure, mass flow rate and quality) to spread CHF across half of the bundle geometry, and over 100% to spread across the whole geometry [4]. The purpose of this study is to qualify and quantify on experimental and modelling bases this three-dimensional spatial dry-out front propagation within a rod bundle during transient condition.

Experimental Approach

In order to investigate detailed thermal hydraulic behaviour of rod bundle geometry during transient events as well as the spatial effects on CHF occurrence and its widening an experimental investigation has been performed by JAERI (Japan Atomic Energy Research Institute).

Apparatus and Conditions

The bundle test section consisting of 15 heated rods and one non-heated rod is shown in Figure 1, together with all measured parameters. The heated rods are indirectly heated by electrical heaters and simulate BWR nuclear fuel rods. They are supported to keep appropriate horizontal position by seven spacers (Figure 2). The shape of the spacers is designed to simulate those used in BWRs. The pitch of the rods (16.3 mm), the outer diameter (12.3 mm) and the heated length (3.71 m) of the rods are equal to those of modern BWR bundles. The axial power shape is chopped cosine with the peaking factor of 1.40. By controlling the electrical input to the power units (each consists of 3 rods and are presented in Figure 3) the radial power distribution can be varied. Clad temperature is measured with 8 azimuthally placed thermo-couples at each of 14 axial elevations, shown in Figure 2.

Demonstration Transient

The experiment used in this analysis simulates an event of a BWR Turbine Trip without By-Pass (TTw/oBP). According to the safety evaluation analysis, a decrease in steam removing, after the transient initiation, results in a pressure rise in the reactor pressure vessel. This results in reduction of void fraction, and an increase of the core power up to the level that causes hydraulic scram and reactor shutdown followed by core power reduction to decay heat. Due to the core power increase re-circulation pumps are stopped reducing then the core flow rate.
According to the conventional reactor design, a reactor is shutdown at 108% of the rating power. Typical event of TTw/oBP is characterised with no rods in film boiling and without occurrence of core heat up. However, in this experiment the core shutdown (power reduction) was intentionally delayed

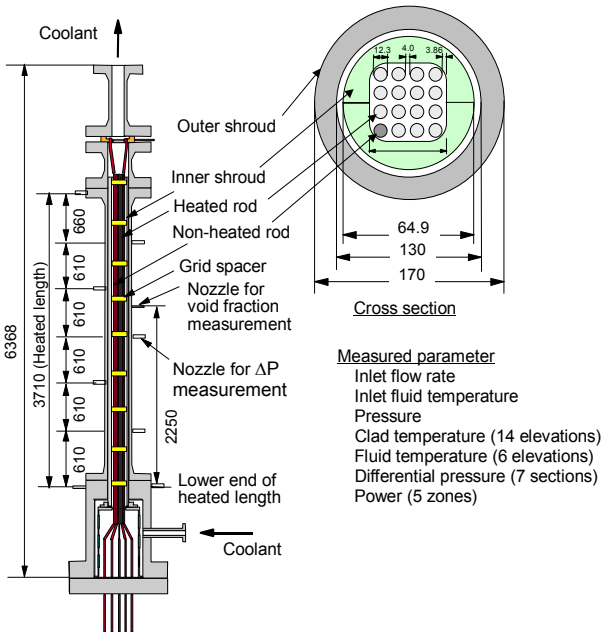

Figure 1. 4x4 rod bundle test section

✧Temporarily at Framatome ANP GmbH, P.O.Box 3220, D-91050 Erlangen, Germany
□A.T.H.A. – Advanced Thermal Hydraulics with Applications. e-Mail: Zoran@Stosic.de , URL: http://www.Stosic.de

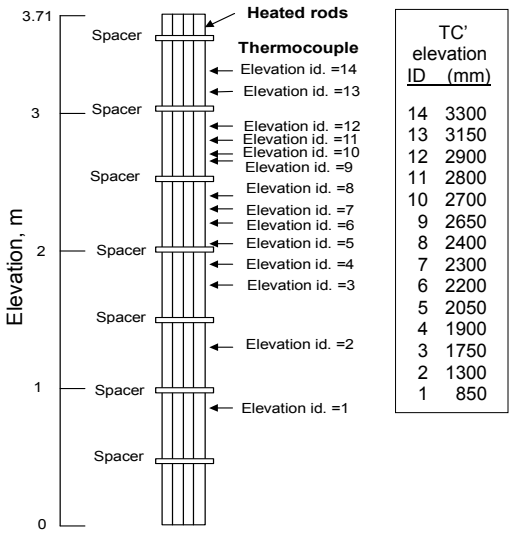

Figure 2. Positions of spacers and thermocouples

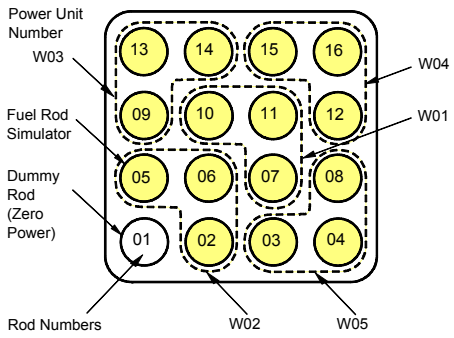

Figure 3. Layout of power units and rod numbering

in order to realize post dry-out regime and the rod bundle heat up, reaching the maximum power value equals to 192% of rating one. Measured variations of parameters are given in Figure 4.

Applied Model

Three-dimensional coolant two-phase flow within the bundle is modelled by the "three-fluid" model approach [8]. Fluid flow conservation equations are written for both phases and three fluid streams.

Objectives

The porous medium concept is used in the simulation. The space of the control volume can be occupied by one, two or three fluid streams as well as by rods and/or spacers. Flow resistance is assumed to be continuously distributed in the space occupied by these elements. Governing equations are written in the non-viscous form, while the turbulent viscosity effects are considered indirectly through friction coefficients for the tube bundles flow resistance and two-phase interfacial drag forces. The two-phase flow is observed as semi-compressible. The surface tension is neglected, as not important for bulk two-phase flow. Heating entrance section of the bundle, up to the incipience of boiling, is modelled only by the one-fluid approach. Subsequent bubbly, churn or slug flow patterns are modelled by the two-fluid model concept with the conservation equations for liquid and vapour phase. The annular flow pattern is reached when the steam void α_2>0.3 and the vapour superficial velocity exceeds the value 15 m/s, and it is modelled by the three-fluid model written for liquid film on the rod wall, entrained liquid droplets and vapour core.

Governing Equations

Liquid continuous phase or droplets mass conservation (the last term on the r.h.s. is included in case of droplets flow)

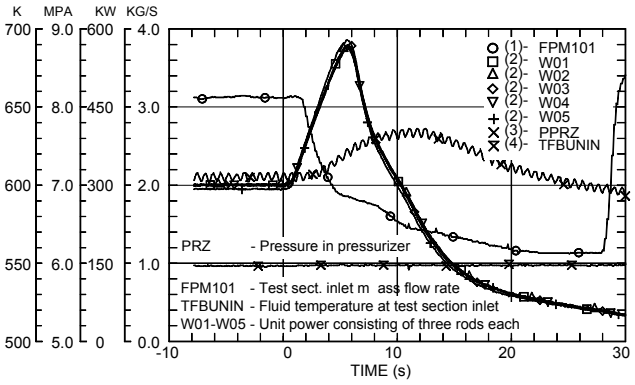

Figure 4. Measured variation of inlet and boundary conditions during TTw/oBP transient simulation

$$\frac{\partial(\alpha_1\rho_1)}{\partial t}+\nabla\cdot(\alpha_1\rho_1\vec{u}_1)=-\Gamma_{12}+\Gamma_{21}-\frac{S}{A}(W_d-W_e) \quad (1)$$

Vapour mass conservation

$$\frac{\partial(\alpha_2\rho_2)}{\partial t}+\nabla\cdot(\alpha_2\rho_2\vec{u}_2)=\Gamma_{12}-\Gamma_{21}+\Gamma_{32}-\Gamma_{23} \quad (2)$$

Liquid film mass conservation

$$\frac{\partial(\alpha_3\rho_3)}{\partial t}+\frac{\partial(\alpha_3\rho_{31}u_3)}{\partial z}=-\Gamma_{32}+\Gamma_{23}+\frac{S}{A}(W_d-W_e) \quad (3)$$

Liquid continuous phase or droplets momentum conservation (the last term on the r.h.s. is included in case of droplets flow)

$$\frac{\partial(\alpha_1\rho_1\vec{u}_1)}{\partial t}+\nabla\cdot(\alpha_1\rho_1\vec{u}_1\vec{u}_1)=-\alpha_1\nabla p+\alpha_1\rho_1\vec{g}-\vec{F}_{L2}+\vec{F}_{VM}$$
$$+\vec{F}_{21}-\vec{F}_{41}-\Gamma_{12}\vec{u}_1+\Gamma_{21}\vec{u}_2-\frac{S}{A}(W_d u_{1,Z}\vec{k}-W_e\vec{u}_3) \quad (4)$$

Vapour momentum conservation

$$\frac{\partial(\alpha_2\rho_2\vec{u}_2)}{\partial t}+\nabla\cdot(\alpha_2\rho_2\vec{u}_2\vec{u}_2)=-\alpha_2\nabla p+\alpha_2\rho_2\vec{g}+$$
$$\vec{F}_{L2}-\vec{F}_{VM}-\vec{F}_{21}-\vec{F}_{23}-\vec{F}_{42}+$$
$$\Gamma_{12}\vec{u}_1-\Gamma_{21}\vec{u}_2+\Gamma_{32}\vec{u}_3-\Gamma_{23}\vec{u}_2 \quad (5)$$

Liquid film momentum conservation

$$\frac{\partial(\alpha_3\rho_3\vec{u}_3)}{\partial t}+\nabla\cdot(\alpha_3\rho_3\vec{u}_3\vec{u}_3)=-\alpha_3\nabla p+\alpha_3\rho_3\vec{g}-\vec{F}_{23}-\vec{F}_{43}$$
$$-\Gamma_{32}\vec{u}_3+\Gamma_{23}\vec{u}_2+\frac{S}{A}(W_d u_{1,Z}\vec{k}-W_e\vec{u}_3) \quad (6)$$

Liquid continuous phase or droplets energy conservation (the last term on the r.h.s. is included in case of droplets flow)

$$\frac{\partial(\alpha_1\rho_1 h_1)}{\partial t}+\nabla\cdot(\alpha_1\rho_1 h_1\vec{u}_1)=-(\Gamma_{12}-\Gamma_{21})h''+$$
$$\dot{q}'''_{41}-\frac{S}{A}(W_d h_1-W_e h_3) \quad (7)$$

Vapour energy conservation

$$\frac{\partial(\alpha_2\rho_2 h_2)}{\partial t}+\nabla\cdot(\alpha_2\rho_2 h_2\vec{u}_2)=(\Gamma_{32}-\Gamma_{23})h''+(\Gamma_{12}-\Gamma_{21})h'' \quad (8)$$

Liquid film energy conservation

$$\frac{\partial(\alpha_3\rho_3 h_3)}{\partial t}+\nabla\cdot(\alpha_3\rho_3 h_3\vec{u}_3)=-(\Gamma_{32}-\Gamma_{23})h''+$$
$$\dot{q}'''_{43}+\frac{S}{A}(W_d h_1-W_e h_3) \quad (9)$$

The source terms for mass, momentum and thermal energy conservation are written on the r.h.s. of Eqs. (1) – (9). The intensity of phase transition, which is the mass of evaporation or condensation per unit volume and time, is denoted with Γ. The interfacial drag forces per unit volume for vapour and continuous

liquid or droplets drag are denoted with $\vec{F}_{21}$, and with $\vec{F}_{23}$ for vapour and liquid film drag. Wall-vapour friction force is $\vec{F}_{42}$, wall-continuous liquid or droplets $\vec{F}_{41}$, and wall-liquid film $\vec{F}_{43}$. Terms $\vec{F}_{L2}$ and $\vec{F}_{VM}$ represent lift force and virtual mass force, respectively. The term $\dot{q}_{4k}$ represents volumetric heat rate from rods to corresponding fluid phase per unit volume.

Closure Laws

The necessary closure laws for the calculation of these terms are presented in [3, 5]. The deposition rate is calculated with the correlation for the deposition coefficient in steam-water two-phase flow from [2]. Entrainment rate is predicted with correlation from [10]. To the above equations is added:

Volume fraction balance

$$\alpha_1 + \alpha_2 + \alpha_3 + \alpha_4 = 1 \qquad (10)$$

where indexes 1, 2, 3 and 4 denote continuous liquid phase or entrained droplets, vapour phase, liquid film on the wall and rods and/or spacers respectively.

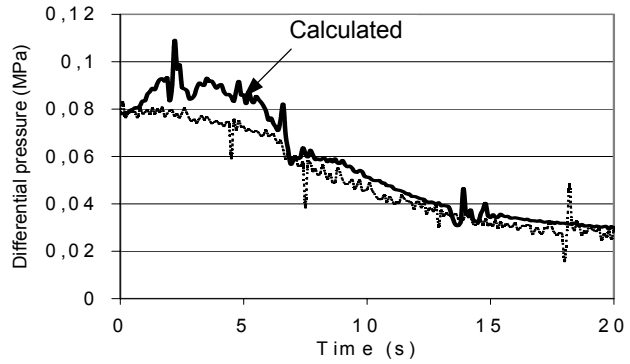

Figure 5. Measured and calculated pressure drop along the rod bundle during TTw/oBP transient simulation

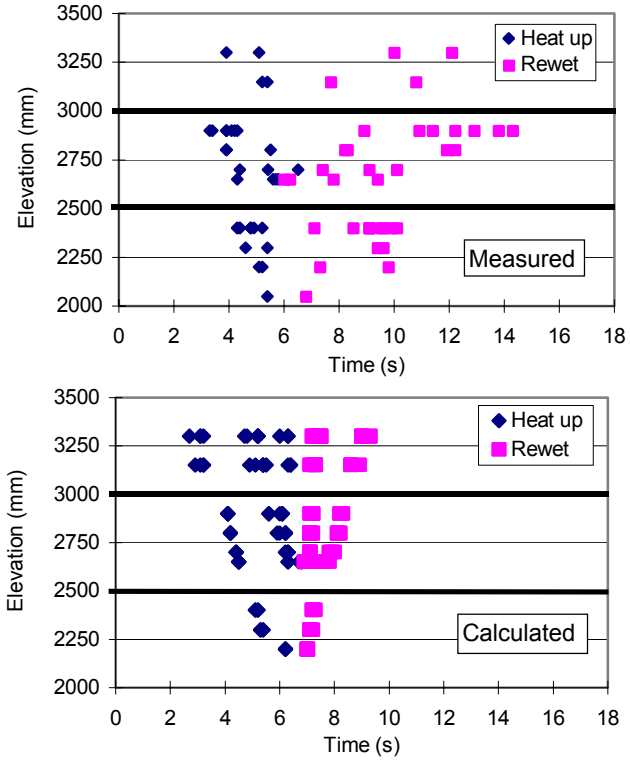

Figure 6. Measured (top) and calculated (bottom) data indicating axial propagation of CHF/Rewetting front during TTw/oBP transient simulation

Simplified Dryout Criteria

The dry-out criteria for churn-turbulent two-phase flow, assumed to prevail for steam voids α_2>0.3 and steam superficial velocities lower than 15 m/s [5, 6], is the condition under which the steam void fraction reaches the value of 0.98 [9].

For annular flow, it is adopted that the dry-out occurs when the complete liquid film depletion happens. The complete film disappearance is triggered at the minimum possible film thickness assumed to be equal to or less than 10 microns, which has already been successfully applied and verified [7, 8].

Results and Discussion

Regarding predefined variation of inlet and boundary conditions (Figure 4) experimental and numerical investigation of three-dimensional propagation of CHF/rewet front during simulation of TTw/oBP transient have been performed. Numerical analyses based on described porous media concept have been done modelling the 4x4 rod bundle (Figure 1) by 4x4x58 (928) nodes (in axial direction 58 nodes were used).

Figure 5 shows satisfactory agreement between measured and calculated total pressure drop along the rod bundle during analysed transient simulation (Figure 4).

Measured data of dry-out front propagation down the bundle and rewetting locus are shown in Figure 6 (top). As effect of spacers the duration of post dry-out phase is the shortest just downstream of the grid increasing with the height and reaching the maximum just upstream of the next spacer grid. With time marching the CHF initiates first upstream of the spacers propagating upstream to the lower elevation grid, while rewetting occurs just behind the spacer grids propagating downstream. This means that there are time sequences with more than one CHF (Figure 6 at about 4-5 sec) and more than one axial locus of rewetting (Figure 6 for about 8-10 sec). The later one is less steep and existence of more than one rewetting front is characteristic for coolant high flow rate and high power generation [1, 4].

Calculated data of dry-out/rewetting axial propagation during analysed transient are presented in Figure 6 (bottom). Onset of CHF is predicted to occur 0.6 sec before the measured one. The CHF front propagation down the bundle is calculated to end 0.5 sec later than measured. Bottom rewetting is measured to start at 7.3 sec after transient initiation, while 7 sec is calculated. The calculation shows that complete rewetting occurs about 4 sec earlier than measured. Minimum height of the CHF front is calculated to be only 150 mm higher than the measured one, which was indicated only by two thermocouples at side rods.

Figure 7 illustrates spatial distribution of calculated void fraction at 1.1 sec after onset of the dry-out.

Measured data of CHF lateral propagation (based on clad temperature excursion) as well as calculated values (based on

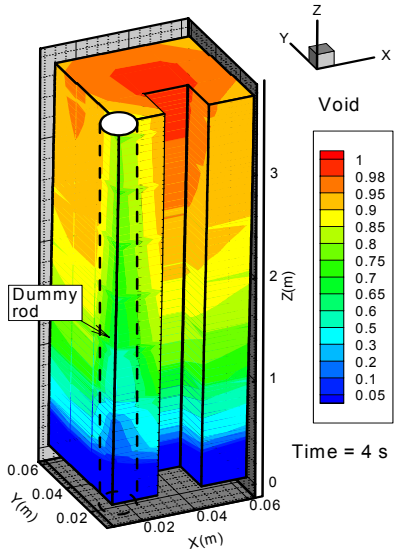

Figure 7. Calculated void fraction distribution at 4 sec. after the start of TTw/oBP transient (1.1 sec after dry-out initiation)

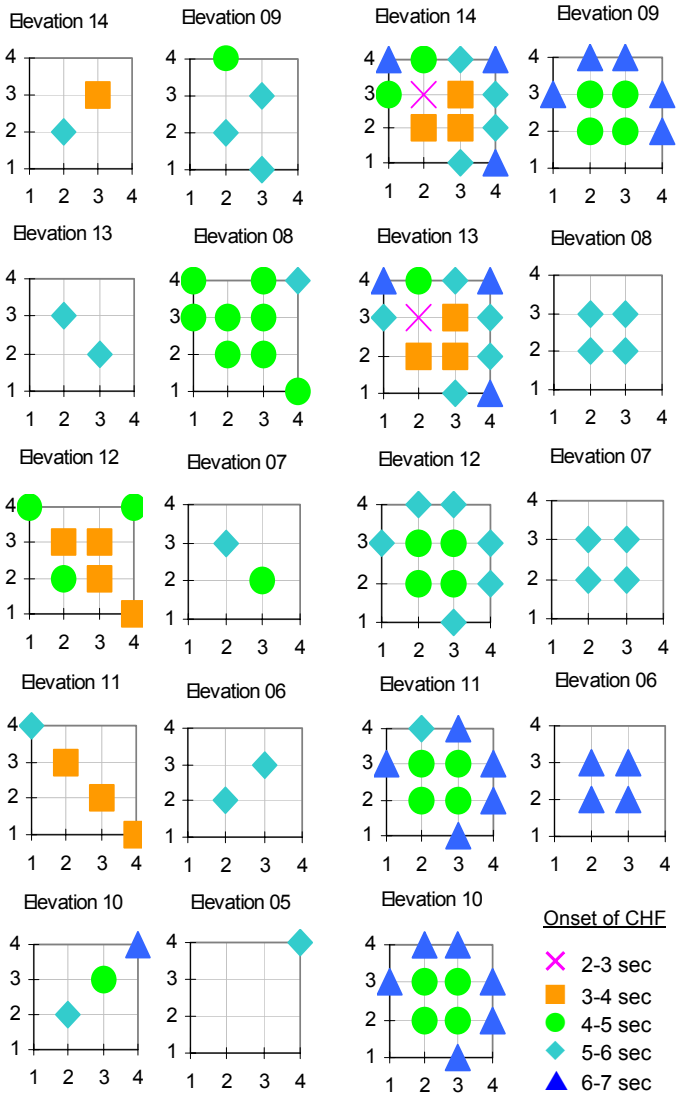

Figure 8. Measured (left) and calculated (right) data indicating lateral propagation of CHF on different elevations during TTw/oBP transient simulation

introduced dry-out criteria) across the bundle on different elevations during simulated transient are shown in Figure 8. Presented measured data indicate that the CHF is spread across almost the whole bundle on elevation 8 after 5 to 6 seconds after transient initiation when the power generation has reached 192% of nominal value. The exceptions are dummy rod with three neighbours and three side rods opposite to it, as shown in Figure 8. This lateral propagation of CHF front corresponds roughly to the percentage of power increase over the bundle critical value [4] initiated after 3.3 seconds on elevation 12. The first CHF on elevation 8 has been detected 1 second later, i.e. in 4.3 seconds after transient initiation.

The numerical results of lateral spreading of the CHF zone across the bundle have shown that more rods have been dried-out at height upstream the elevation 8 compared to number of powered rods measured experiencing heat-up (post-CHF) condition. One of the reason is the fact that in the rod bundle test section not all of the rods at all elevations have been mounted with thermocouples. For instance, at elevations 06, 07, 10, 13 and 14 only three rods were mounted with thermocouples, i.e. rods 06, 11, 16 (Figure 3) at elevations 06, 10 and 14 and rods 07, 10 and 15 at elevations 07 and 13. At elevation 08 all rods except 01, 03, 05, 12, and 14 (Figure 3) were mounted with thermocouples.

Generally, the obtained disagreements between calculated and measured three-dimensional CHF/rewet front propagation are direct consequences of implemented simple dry-out criteria with no effects of the local velocities of fluid streams (already shown to have an influence in both 2-fluid [9] and 3-fluid [8] fields) as well as numerical simulation performed without rod model.

Conclusions

Experimental and numerical (three-dimensional three-fluid model based on porous media approach) investigation of spatial propagation of CHF/rewet front within nuclear fuel rod bundle under transient condition is performed.

There are time sequences with more than one CHF and/or rewetting front influenced by spacers. The CHF initiates first upstream of the spacers propagating upstream to the lower elevation grid, while rewetting occurs just behind the spacer grids propagating downstream. Special emphasis is given to the lateral CHF propagation, i.e. the influence of transient power increase on spreading the CHF condition across the bundle. It is found that this spreading is more or less proportional to the power increase over the bundle critical power value.

Best estimate numerical simulation has indicated transient spatial thermal hydraulics and resultant 3D propagation of CHF/rewet front within the 4x4 rod bundle with encouraging agreements. It has to be noted that simple dry-out criteria and no rod model in current porous media approach cause differences between calculated and measured CHF/rewetting behaviour.

Thermal hydraulic of spatial enhancement of CHF locus has to be investigated further in regard to possible formation of vapour zone within the bundle with increased heat-up consequences.

References

[1] Iguchi, T., et al., Result of Reflood Experiment with 5x5 Bundle Test Section under Wide Pressure Condition. *ICONE-6: 6th ASME/SFEN/JSME Int. Conference on Nuclear Engineering*, San Diego, USA, May 10-15, 1998.

[2] Saito, T., Hughes, E. D. and Carbon, M. W., Multi-fluid Modelling of Annular Two-Phase Flow, *Nuclear Engineering and Design*, **50**, 1978, 225-271.

[3] Stevanovic, V. et al., A Simple Model for Vertical Annular and Horizontal Stratified two-phase flows with liquid entrainment and phase transitions: one-dimensional steady state conditions, *Nuclear Engineering and Design*, **154**, 1995, 357-379.

[4] Stosic, Z., On the Role of Spacer Grids on of Dryout/Rewetting on local Thermal Hydraulics in Boiling Water Channels, *9th Int. Topical Meeting on Nuclear Reactor Thermal Hydraulics – NURETH-9*, San Francisco, USA, October 3-9, 1999.

[5] Stosic, Z. and Stevanovic, V., An Advanced Numerical Method for Transient Multidimensional Two-Phase Flow Thermal-Hydraulics in Complex Geometry with Rod or Tube Bundles, *Int. Symposium on Advanced in Computational Heat Transfer*, Palm Cove, Queensland, Australia, May 20-25, 2001.

[6] Stosic, Z. and Stevanovic, V., A Three-Dimensional Numerical Investigation of Two-Phase Flow Thermal-Hydraulics within Advanced Nuclear Fuel Rod Bundles, *Int. Symposium on Advanced in Computational Heat Transfer*, May 20-25, Palm Cove, Queensland, Australia, 2001.

[7] Stosic, Z. and Stevanovic, V., Schematisation of the Multi-Fluid Approach and Its Application to the CHF Prediction, *4th Int. Conference on Multiphase Flow*, May 27-June 1, New Orleans, Louisiana, USA, 2001.

[8] Stosic, Z. and Stevanovic, V., A Detailed Three-Dimensional Three-Fluid Numerical Investigation of Two-Phase Flow in Complex Geometry based on the Porous Media Concept: Critical Heat Flux Predictions, *1st Int. Conference on Heat Transfer, Fluid Mechanics and Thermodynamics – HEFAT-2002*, April 8-10, Kruger Park, South Africa, 2002.

[9] Stosic, Z., Stevanovic, V. and Iguchi, T., Three-Dimensional Porous Media based numerical Investigation of Spatial Power Distribution Effect on Advanced Nuclear Fuel Rod Bundles Critical Power, *2nd Int. Conference on Computational Heat and Mass Transfer*, October 22-26, Rio de Janeiro, Brazil, 2001.

[10] Sugawara, S., Droplet Deposition and Entrainment Modelling Based on the Three-Fluid Model, *3rd Int. Topical Meeting on Nuclear Power Plant Thermal Hydraulics and Operation*, Seoul, Korea, 1988, A1-19-28.